Refolding of Thermally and Urea-Denatured Ribonuclease A Monitored by Time-Resolved FTIR Spectroscopy†

Diane Reinstädler,‡ Heinz Fabian,*,§ Jan Backmann,|| and Dieter Naumann*,‡

Robert Koch-Institut, Fachgebiet 311, Postfach 650280, D-13302 Berlin, Germany, Institut für Biochemie, Humboldt-Universität Berlin, c/o Max-Delbrück-Centrum für Molekulare Medizin, Robert-Rössle-Strasse 10, D-13125 Berlin, Germany, and Vrije Universiteit Brussel, ULTR, Paardenstraat 65, B-1640 Sint-Genesius-Rode, Belgium

Received July 22, 1996; Revised Manuscript Received October 2, 1996⊗

ABSTRACT: We undertook a first detailed comparative analysis of the refolding kinetics of ribonuclease A (RNase A) by time-resolved Fourier transform infrared spectroscopy. The refolding process was initiated either by applying a temperature jump on the thermally denatured protein or by rapid dilution of a concentrated [^{13}C]urea solution containing the chemically unfolded protein. The dead time of the injecting and mixing devices and the time-resolution of the spectrometer permitted us to monitor the refolding kinetics in a time range of 100 ms to minutes. The infrared amide I′ band at 1631 cm^{-1} was used to directly probe the formation of β-sheet structure during the refolding process. The aromatic ring stretching vibration of tyrosine at 1515 cm^{-1} was employed as a local monitor that detects changes in the tertiary structure along the folding pathway. The comparative analysis of the kinetics of the β-sheet formation of chemically and thermally denatured ribonuclease A revealed similar folding rates and amplitudes when followed under identical refolding conditions. Therefore, our kinetic infrared studies provide evidence for a high structural similarity of urea-denatured and heat-denatured RNase A, corroborating the conclusions derived from the direct comparison of the infrared spectra of thermally and chemically denatured RNase A under equilibrium conditions [Fabian, H., & Mantsch, H. H. (1995) *Biochemistry 34*, 13651−13655]. In detail, the kinetic infrared data demonstrate that in the time window of 0.1−30 s approximately 40% of the native β-sheet structure in RNase A is formed in the presence of 0.6 M urea at pH* 3.6, indicating that up to 60% of the β-structure is formed out of the time window used in this study. Temperature jump experiments in the absence of chemical denaturants exhibited faster and more complex refolding kinetics. In addition, differences in the time constants of refolding derived from the amide I′ band at 1631 cm^{-1} and from the tyrosine vibration at 1515 cm^{-1} were observed, indicating that the formation of secondary structure precedes the formation of stable tertiary contacts during the refolding of RNase A.

One of the most sophisticated problems of protein chemistry concerns the pathway of protein folding, i.e., the spontaneous transition of the polypeptide chain from a quasi-random state to its unique three-dimensional structure. It is well-known that a random search of the peptide chain through all possible conformational states during the folding process does not occur. This would exceed most biological lifetimes (Levinthal, 1968). Even though the information guiding the molecule to its native conformation must be encoded in the primary structure, the prediction of the 3D structure from the knowledge of the amino acid sequence alone is still a scientific challenge [for a review, see Fischer et al. (1996)]. Solving the problem of protein folding, that is, to characterize all intermediates and activated states of a given folding pathway and arrange them in their correct order (Schmid, 1992), would be a great step toward this aim. Because of the complexity of living cells, the study of folding behavior of proteins *in vivo* is extremely obstructed. The general approach is to observe these events on isolated systems *in vitro*, usually with small globular proteins as model systems. In this way, a great variety of techniques has been used to follow the folding process, including nuclear magnetic resonance (NMR)[1] spectroscopy in combination with pulse-labeling methods (Schmid & Baldwin, 1979; Udgaonkar & Baldwin, 1988, 1990, 1995; Jeng et al., 1990; Mullins et al., 1993), real time NMR (Akasaka et al., 1991; Balbach et al., 1995), CD, UV absorbance, and fluorescence (Cook et al., 1979; Chaffotte et al., 1992; Houry et al., 1994; Dodge & Scheraga, 1996). In most of these investigations, the proteins were unfolded by chemical denaturants (e.g., urea or guanidinium chloride), and refolding was initiated by rapid dilution applying stopped-flow techniques. NMR spectroscopy plays a prominent role in these investigations due to its ability to follow protein folding at an atomic level.

Fourier transform infrared (FTIR) spectroscopy has proved to be a powerful tool for following conformational changes in proteins under equilibrium conditions [for a review, see Jackson and Mantsch (1995)]. Peptide backbone and side-chain infrared "marker" bands were employed as conformation-sensitive monitors (Fabian et al., 1993, 1994). Very recently, techniques have been developed to follow processes of unfolding or refolding in proteins initiated by temperature

† This work was supported by the Deutsche Forschungsgemeinschaft (Grant Na226/3-3).

* Correspondence should be addressed to either of these authors.
‡ Robert Koch-Institut.
§ Humboldt-Universität Berlin.
|| Vrije Universiteit Brussel.

⊗ Abstract published in *Advance ACS Abstracts,* November 1, 1996.

[1] Abbreviations: RNase A, ribonuclease A; FTIR, Fourier transform infrared; TRIR, time-resolved infrared; T-jump, temperature jump; NMR, nuclear magnetic resonance; CD, circular dichroism; pH*, glass electrode pH reading in D_2O solutions without correction for isotope effects; AU, absorbance units.

S0006-2960(96)01810-7 CCC: $12.00

jump (T-jump) using time-resolved infrared (TRIR) spectroscopy. Thermally induced unfolding of RNase A (Phillips et al., 1995) or helix melting in a small peptide (Williams et al., 1996) after applying laser-induced T-jumps was monitored by TRIR spectroscopy on the picosecond/nanosecond time scale. In another approach, a fast injection attachment was developed to follow refolding of RNase A after thermal denaturation on the millisecond to minute time scale with FTIR spectroscopy (Backmann et al., 1995). In addition, a stopped-flow apparatus was developed for infrared spectroscopy (White et al., 1995) that may serve as a prototype for a mixing device permitting the investigation of unfolding and refolding processes in proteins initiated by chemical denaturants.

Herein, we investigate for the first time the refolding kinetics of a chemically denatured protein with time-resolved FTIR spectroscopy after rapid dilution of a highly concentrated ^{13}C-labeled urea solution in a stopped-flow apparatus. In a second type of experiment, the refolding process from the thermally denatured state is initiated by applying a T-jump. The protein we have chosen, RNase A, is a single-domain protein that has frequently served as model protein in folding studies (Cook et al., 1979; Udgaonkar & Baldwin, 1988). Furthermore, in contrast to many other proteins, the thermal unfolding of RNase A is reversible even at the high protein concentrations required for infrared experiments.

It is still a topic of discussion whether there are conformational differences between heat-denatured and chemically denatured RNase A in particular, and between the corresponding states of proteins in general. Often, the use of chaotropic agents such as urea and guanidine hydrochloride is reported to be more effective in protein unfolding than temperature (Tanford, 1968). However, recent comparative infrared studies revealed at the level of secondary structure no differences between heat-denatured and urea-denatured RNase A under equilibrium conditions (Fabian & Mantsch, 1995). Herein, we present a different approach to address this question by comparing its refolding kinetics starting from the thermally unfolded and the chemically unfolded state, respectively. Possible differences between heat-denatured RNase A and chemically denatured RNase A should result in different refolding kinetics. In the absence of such conformational differences, practically identical refolding kinetics are expected. To the best of our knowledge, this is the first comparative investigation of protein refolding after chemical and thermal denaturation.

MATERIALS AND METHODS

Materials. Highly purified lyophilized RNase A from bovine pancreas (type XII-A) and [^{13}C]urea (99 atom % ^{13}C) were purchased from Sigma Chemie GmbH (Deisenhofen, Germany). Deuterated [^{13}C]urea was prepared by repeated lyophilization of [^{13}C]urea from a D_2O solution.

Measurements under Equilibrium Conditions. All infrared spectra were recorded using a Bruker IFS-66 FTIR spectrometer. To eliminate spectral contributions due to atmospheric water vapor, the instrument was continuously purged with dry air. Infrared spectra under equilibrium conditions were recorded using a DTGS detector.

Solutions containing deuterated [^{13}C]urea in the range of 0−8 mol/L were prepared volumetrically by mixing freshly made 8 M urea/D_2O stock solutions and pure D_2O at pH* 3.6 according to Pace (1986). The use of ^{13}C-labeled urea for the infrared experiments was essential, since it causes the C═O band of urea to shift well below 1600 cm^{-1} and, in this way, permits analysis of the amide I band of the protein (Fabian & Mantsch, 1995). RNase A was dissolved in 20 mM sodium citrate/D_2O buffer at pH* 3.6, heated for 15 min at 60 °C to achieve complete H/D exchange of the amide protons, and cooled down to room temperature. After lyophilization, deuterated RNase A was dissolved in 20 μL of the corresponding solvent to obtain a concentration of ∼25 mg of enzyme/mL. The protein was allowed to equilibrate for at least 10 h at 4 °C before the measurements. The protein solutions containing different urea concentrations were placed between a pair of CaF_2 windows separated by a path length of 6 μm. For proper compensation of D_2O and denaturant absorption, the corresponding solvents were placed in the same cell but with slightly shorter (1−2%) path lengths. Solvent spectra were recorded under identical conditions and were subtracted from the corresponding protein spectra. For each measurement, 256 interferograms were co-added and Fourier-transformed employing a Boxcar apodization function to yield spectra with a nominal resolution of 4 cm^{-1}.

For the temperature profile measurements, infrared spectra were collected continuously in a thermostated IR cuvette with an optical path length of 50 μm. Completely H/D-exchanged RNase A was dissolved in 20 mM sodium citrate/D_2O buffer at pH* 3.8 to obtain a protein content of ∼20 mg/mL. The protein was unfolded and refolded by exposing it to a linear temperature gradient from 20 to 80 °C and back to 20 °C at a rate of 0.5 K/min. All protein spectra were corrected for the contributions of buffer as described previously (Fabian et al., 1993).

Kinetic Measurements. All kinetic experiments were performed using a Bruker IFS-66 FTIR spectrometer equipped with a liquid nitrogen cooled HgCdTe detector. Nominal physical resolution was 4 cm^{-1}; the encoding interval of data points was approximately one point per wavenumber. Due to the parameters chosen for these particular experiments (resolution 4 cm^{-1}, scanner velocity 100 kHz, double-sided acquisition mode), one scan took 71 ms in the *Rapid Scan* mode, and two successive scans were effectively separated by a time interval of 95 ms. The sum of both defines the actual time-resolution of the experimental setup. The dead time of sample injection was estimated to be on the order of 30 ms, which is shorter than the instrumental dead time of 100 ms. Due to the capacity of the acquisition processor, which allowed collection of 186 single-beam interferograms, the duration of data collection was restricted to 30 s. The interferograms were converted to single-beam spectra using a Blackman-Haris-3-Term apodization function. The difference spectra were calculated from the common logarithm of the ratio of the last single-beam spectrum and a running single-beam spectrum. Absorbance changes were evaluated directly from these difference spectra. Since it is difficult to derive peak shifts from difference spectra, the frequency of the tyrosine band at ∼1515 cm^{-1} was determined from the second derivatives of the single-beam spectra.

The stopped-flow dilution experiments were carried out using a modified rapid mixing attachment (derived from the SFA-20 model from Hi-Tech Ltd., Salisbury, U.K.) connected with a mixing flow cell developed by Dr. C. W. Wharton, Birmingham, U.K. [see also White et al. (1995)]. For the measurements, our cell was thermostated at 20 °C. To obtain chemically denatured RNase A, the protein (∼110

mg/mL) was kept in the unfolding D_2O buffer containing 6.5 M [^{13}C]urea in 20 mM sodium citrate/D_2O at pH* 3.6 for at least 10 h. The denaturant concentration was reduced under the unfolding concentration by rapid dilution of the protein/urea solution with 10 volumes of urea-free buffer by applying a pneumatic drive. The drive was triggered by an electric signal from the spectrometer. In this way, precise time correlation of data acquisition and mixing time was achieved. Final refolding conditions were ~10 mg/mL protein, 0.6 M [^{13}C]urea, pH* 3.6. To reduce the dead volume of the protein solution, an additional 3-way valve was inserted into the protein flow line, which allows one to push the protein sample immediately in front of the cell's mixing jet. In this way, for each experiment 50 μL of the protein/urea solution was preinjected into the flow line before the pneumatic drive shot 30 μL of the protein solution and 300 μL of the buffer solution into the mixing flow cell.

The T-jump experiments were performed as described recently (Backmann et al., 1995). RNase A was dissolved in 20 mM sodium citrate/D_2O buffer at pH* 3.6 to obtain a protein concentration of ~10 mg/mL. For the T-jump experiments in the presence of urea, the protein was dissolved in the same buffer but containing 0.6 M [^{13}C]urea. These solutions were kept for 10 min in the injecting syringe which was thermostated at 80 °C, well above the phase transition temperature. To initiate refolding of the thermally unfolded protein, 80 μL of the protein solution was injected into the IR cell that was thermostated at 20 °C.

Software used for analysis of the crystallographic data and visualization were the CCP4 Program Suite, 1994, incl. CContacts Vers. 2.15 and RasMol Vers.2.5, respectively.

RESULTS

First of all, FTIR spectra of RNase A at different concentrations of [^{13}C]urea as well as along a linear temperature gradient were recorded under equilibrium conditions to set up the optimal conditions for the kinetic experiments and to aid the interpretation of the spectral changes.

Chemical Denaturation of RNase A. RNase A was exposed to 14 different [^{13}C]urea concentrations in the range of 0−8 mol·L^{-1}. Measurements were performed after an equilibration period of at least 10 h at 4 °C at the corresponding urea concentration. Figure 1A shows representative infrared spectra of RNase A in D_2O buffer (pH* 3.6) after complete H/D exchange and subtraction of the corresponding solvent spectra. The infrared absorption bands of fully deuterated, ^{13}C-labeled urea at 1561 and 1462 cm^{-1} mask both the amide II′ region and the amino acid side-chain absorptions between 1600 and 1400 cm^{-1}. Therefore, only the amide I′ region of the spectrum of RNase A is shown in Figure 1. Small irregularities in the IR spectra of RNase A below 1620 cm^{-1} may result from insufficient denaturant compensation due to unavoidable minor differences in the urea concentration present in the protein and in the reference solution. In the absence of urea, the infrared spectrum of RNase A is dominated by an amide I′ band contour centered at 1636 cm^{-1}, indicating the presence of β-strands in the native protein (Olinger et al., 1986; Haris et al., 1986). The spectra measured between 0 and 3.5 M urea are very similar to each other, suggesting only small changes in the secondary structure over this urea concentration range. On the other hand, the difference of the spectra measured between 3.5 and 6 M urea clearly demonstrates that the major structural changes occur in this denaturant range. The spectrum obtained after complete chemical denaturation, at 8 M urea, exhibits only a broad, featureless amide I′ band contour centered at 1649 cm^{-1}. This contour is typical of an irregular protein structure.

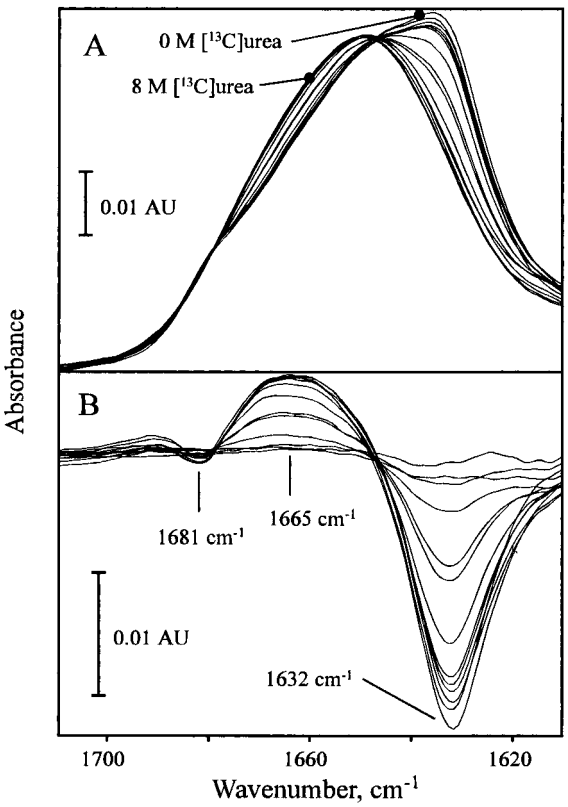

FIGURE 1: Infrared spectra in the amide I′ region of RNase A in D_2O buffer (20 mM citrate) at pH* 3.6 in the presence of 0, 1, 2, 2.5, 3, 3.5, 4, 4.5, 5, 5.5, 6, 6.5, 7, and 8 M [^{13}C]urea. (A) Original absorbance spectra after subtraction of the solvent spectra. (B) Difference spectra calculated from the original spectra according to $A_{8M} - A_{nM}$, where A_{8M} is the absorbance spectrum of RNase A in 8 M urea and A_{nM} is the absorbance spectra at an individual lower concentration of urea in the range of 0−7 M. All difference spectra shown in this work were constructed in such a way that native structures appear as bands pointing downward, regardless of whether refolding or unfolding is observed.

To provide a more detailed illustration of the actual spectral changes occurring in dependence on the concentration of the chaotropic reagent, difference spectra were calculated from the original buffer and denaturant corrected spectra by subtracting the spectra of the RNase A in the presence of different [^{13}C]urea concentrations from the spectrum of RNase A in the presence of 8 M urea (Figure 1B). Negative bands at 1632 and 1681 cm^{-1} indicate decreasing amounts of antiparallel β-sheet structures at advancing chemical perturbation. The loss of secondary structure is accompanied by an increase of irregular structure giving rise to a broad positive band around 1665 cm^{-1}. From these data, intensity/urea concentration profiles for the β-structure "marker" band were constructed. Figure 2 shows the corresponding plot for the infrared band at 1632 cm^{-1}. As the urea concentration is increased, the infrared signal decreases as a sigmoidal function of the urea concentration. This behavior and the presence of an isosbestic point at 1647 cm^{-1} in the difference spectra suggest a simple two-state equilibrium between the folded and the unfolded state under thermodynamic control. This conclusion is in full agreement

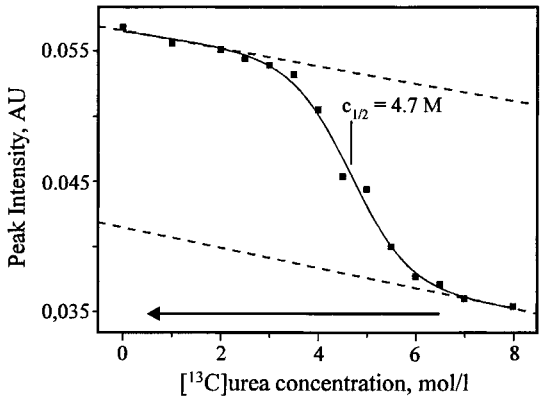

FIGURE 2: Dependence of the peak intensity of the amide I′ band component at 1632 cm^{-1} on the [^{13}C]urea concentration. The experimental values (n) were evaluated from the absorbance spectra after correction of the buffer/denaturant contribution. The solid line represents a Gaussian fit to the experimental points. The horizontal arrow indicates the extent of the urea concentration change during the stopped-flow experiments.

with the results derived from calorimetric, UV, or CD experiments [see, e.g., Pace et al. (1990)]. The transition midpoint concentration of urea ($c_{1/2}$) of 4.7 mol/L as estimated from our measurements in D_2O buffer is almost 1 mol/L higher than that derived from fluorescence data of RNase A in H_2O buffer (Pace et al., 1990), most likely due to isotope effects as discussed below.

Unfolding/Refolding of RNase A along a Linear Temperature Gradient. In order to monitor the thermal unfolding and refolding of RNase A under thermodynamic control, infrared spectra were collected along a linear temperature gradient of 0.5 K·min^{-1} during a heating and cooling cycle between 20 and 80 °C. Figure 3A shows the infrared absorbance spectra of the fully H/D-exchanged enzyme when heating the protein sample from 20 to 80 °C. Practically identical spectra at the corresponding temperatures were obtained during the thermal refolding cycle (spectra not shown). The increase in temperature gives rise to characteristic spectral changes. These temperature-induced changes are emphasized in the difference spectra (Figure 3B) which have been calculated according to $A_{80°C} - A_{n°C}$, where $A_{80°C}$ is the absorbance spectrum recorded at 80 °C and $A_{n°C}$ are the absorbance spectra at temperatures between 20 and 79 °C. Two negative bands at 1632 and 1681 cm^{-1} reflect the loss of antiparallel β-sheet structures during the unfolding process. The broad positive band at 1665 cm^{-1} indicates the appearance of unordered structures while the temperature increases. Interestingly, the characteristics of the infrared difference spectra (negative bands at 1632 and 1681 cm^{-1}, a positive band at 1665 cm^{-1}) are very similar for chemical and thermal denaturation (compare Figure 1B and Figure 3B). Moreover, the almost featureless amide I′ contour centered at 1650 cm^{-1} in the spectrum of RNase A at 80 °C suggests the lack of secondary structure at this temperature. In fact, the infrared spectrum of heat-denatured RNase A was found to be practically identical with that obtained for the chemically unfolded protein at 8 M urea, indicating that the different denaturating conditions lead to virtually identical unfolded states of RNase A. Analogous to the urea denaturation experiments, the dominant β-structure "marker" band at 1632 cm^{-1} was used to construct an intensity/temperature plot to monitor the melting of secondary structure (Figure 4, open squares). In addition, the frequency of the aromatic ring vibration of tyrosine at 1515 cm^{-1},

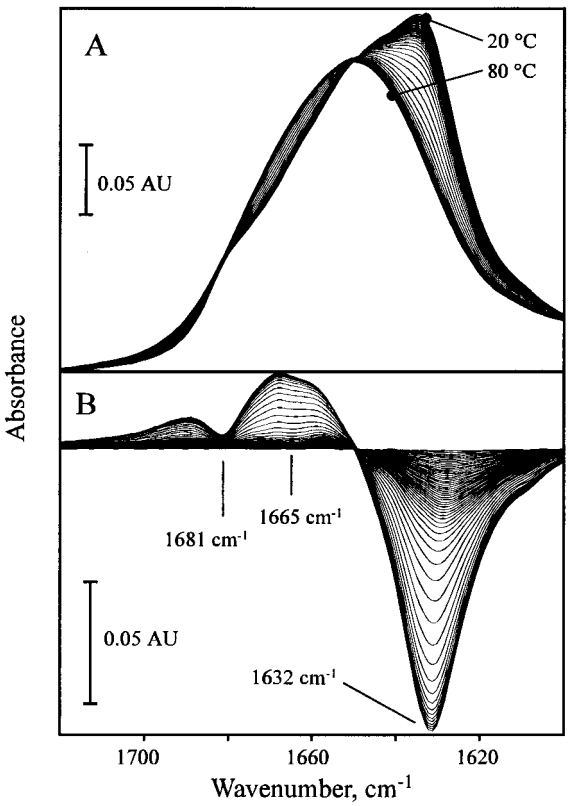

FIGURE 3: Thermal unfolding study of RNase A under the control of linear temperature increase. The temperature was increased from 20 to 80 °C with a constant rate of 0.5 K/min. Since data acquisition took 2 min per spectrum, each spectrum is separated from the next by a temperature step of 1 K. The infrared spectra show the amide I′ region of the enzyme (25 mg/mL RNase A, 20 mM sodium citrate/D_2O buffer, pH* 3.8). (A) Original buffer-corrected absorbance spectra. (B) Difference spectra obtained by calculating $A_{80°C} - A_{n°C}$, where $A_{80°C}$ is the absorbance spectrum recorded at 80 °C and $A_{n°C}$ are the absorbance spectra at the corresponding temperatures between 20 and 79 °C.

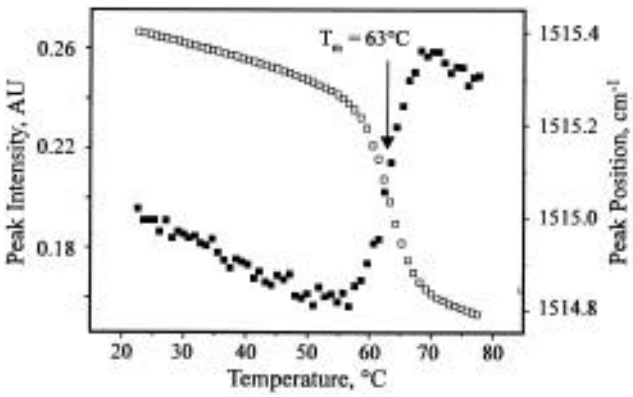

FIGURE 4: Temperature dependence of the peak intensity of the amide I′ band at 1632 cm^{-1} (□) and temperature dependence of the peak position of the tyrosine band (■) for RNase A. The sample was steadily heated from 20 to 80 °C at a rate of 0.5 K/min.

known to be a sensitive local monitor of changes in the microenvironment of tyrosine (Fabian et al., 1994), was used to follow such changes in RNase A. This frequency shift of the tyrosine band with increasing temperature is also shown in Figure 4 (solid squares). The transition curves given in Figure 4 were used to determine the transition temperatures (T_m) and to compute the van't Hoff enthalpies (ΔH_{vH}). Several conclusions can be drawn from these data: (i) The thermal unfolding of RNase A begins near 55 °C and is completed at 70 °C. Below and above the transition

region, the intensity of the β-structure marker band and the frequency of the tyrosine band exhibit a slight, linear decrease with temperature. This effect has already been observed for RNase T1, whose thermal unfolding is also reversible (Fabian et al., 1994). (ii) The T_m values and the transition profiles derived from the two infrared "marker" bands are practically identical ($T_m^{\beta\text{-sheet}} = 63.0$ °C, $T_m^{\text{tyrosine}} = 62.9$ °C, $\Delta H_{vH}^{\beta\text{-sheet}} = -430$ kJ·mol^{-1}, $\Delta H_{vH}^{\text{tyrosine}} = -450$ kJ·mol^{-1}). This indicates the simultaneous breakdown of β-structure elements and changes in the microenvironment of the six tyrosines present in RNase A, suggesting a highly cooperative unfolding process. The fact that the T_m of 63 °C at pH* 3.8 observed herein is about 8−9 °C higher than thermal transition temperatures derived from calorimetric data in H_2O buffer at pH 3.7 (Privalov & Khechinashvili, 1974) can be explained by isotope effects. Generally, the pH in D_2O must be corrected for these effects by adding 0.4 to the pH value measured by the glass electrode (Glasoe & Long, 1960), which corresponds to a pD of 4.2 for our experiments. Furthermore, the thermal transition temperature of RNase A and other proteins in D_2O solutions is about 3−4 °C higher than in H_2O solutions (Makhatadze et al., 1995). Taking both points into account, the T_m value obtained here for RNase A is close to the thermal transition temperatures reported before.

The plots generated from the spectra recorded during the cooling cycle from 80 °C down to 20 °C (not shown) coincide with the data given in Figure 4. The absence of any hysteresis and nearly identical intensity/frequency profiles obtained for the heating and the cooling cycle suggest that the protein is thermally equilibrated at any time during the measurement and that the unfolding of RNase A is completely reversible under our experimental conditions.

Refolding of Chemically Denatured RNase A Monitored by Time-Resolved FTIR Spectroscopy. The use of ^{13}C-labeled urea and the adaptation of stopped-flow techniques permitted us for the first time to monitor the formation of secondary structure in RNase A by TRIR spectroscopy after rapid dilution of the chemically denatured protein. The results obtained from the experiments at discrete urea concentrations were used to set up the conditions for the stopped-flow measurements. The chosen [^{13}C]urea concentration of 6.5 M ensures complete unfolding. After rapid dilution with 10 volumes of urea-free buffer, the final urea concentration (~0.6 M) was well below the transition concentration of $c_{1/2} = 4.7$ M as estimated before (see Figure 2). Figure 5A shows a series of difference spectra of RNase A obtained from a typical stopped-flow dilution experiment. These spectra were calculated from single-beam spectra according to log (S_{last}/S_n), where S_{last} is the spectrum of the last scan and S_n is the spectrum of the nth scan. Decreasing negative band intensities indicate increasing amounts of secondary structure elements after dilution, whereas disappearing positive bands display decreasing amounts of structures populated in the unfolded protein. These difference spectra exhibit striking similarities to those gained from measurements under equilibrium conditions (Figure 1B). Again, a negative band at 1631 cm^{-1}, which dominates the IR difference spectrum, and a weaker component at 1681 cm^{-1} are observed, indicating the formation of antiparallel β-sheet structures after dilution. The broad positive band at ~1665 cm^{-1} reflects the disappearance of different irregular structures.

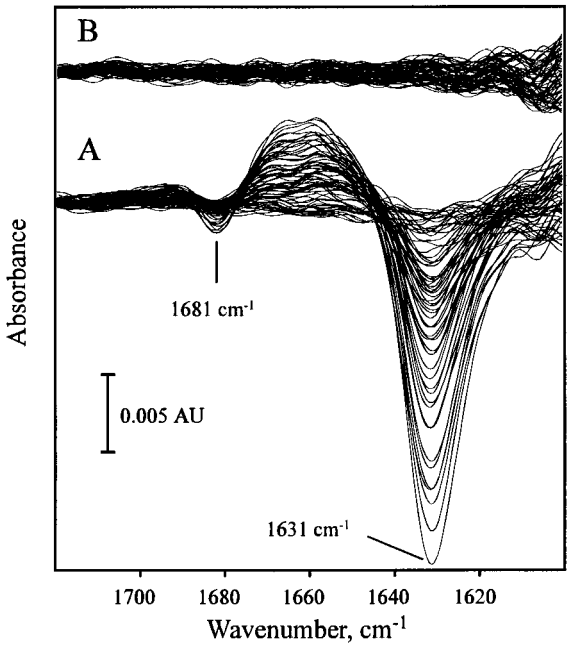

FIGURE 5: Difference spectra obtained from measurements during a [^{13}C]urea dilution experiment using the stopped-flow apparatus. The spectra were calculated from the single-beam spectra according to log (S_{last}/S_n), where S_n is the spectrum of the nth scan and S_{last} is the spectrum of the last scan. Final conditions after dilution: [^{13}C]-urea concentration ~0.6 M, 20 mM sodium citrate/D_2O buffer, pH* 3.6. (A) Refolding experiment with RNase A. (B) Control experiment without protein.

Several control experiments were carried out to ensure that only protein folding events contribute to the spectral characteristics observed in the difference spectra given in Figure 5A. In a first control experiment, only buffer was mixed with buffer using the stopped-flow apparatus in order to test whether subsequent flow or air bubbles could cause base line shifts or spectral interferences. The difference spectra obtained from these experiments only show flat lines, indicating that stable conditions are attained after the mixing event within the experimental dead time of 100 ms. In two further control experiments, a protein/buffer solution and a [^{13}C]urea/buffer solution, respectively, were rapidly diluted with pure buffer under conditions identical to those in the actual refolding experiment. The difference spectra of the latter are depicted in Figure 5B. In comparison to the experiments with pure buffer (data not shown), only an increased noise level below 1620 cm^{-1} due to the strong absorbance of the denaturant is observed. These control measurements certify that spectral artifacts caused by intermolecular interactions or by unstable solvent conditions can be excluded for our stopped-flow experiments.

Refolding Kinetics of RNase A Triggered by a Temperature Jump. In a second type of kinetic experiments, temperature jumps over a range of 60 °C (from 80 °C down to 20 °C) were applied to initiate refolding of the thermally unfolded enzyme. As shown earlier (Backmann et al., 1995), the temperature in the IR cell drops significantly below the transition temperature within the instrumental dead time of 100 ms and stabilizes within the first scans. The first five spectra recorded after the T-jump exhibited characteristics of residual temperature adaptation of the buffer which corresponds to a temperature difference of about 2 K. The affected spectra were corrected for this effect by subtraction of corresponding buffer difference spectra. In order to compare directly the kinetics of temperature-induced refold-

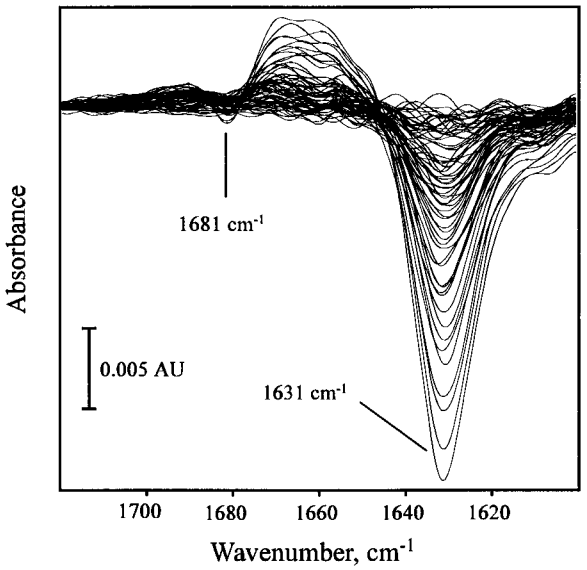

FIGURE 6: Difference spectra of RNase A in 20 mM sodium citrate/D_2O buffer (pH* 3.6) obtained from measurements with RNase A during a T-jump experiment from 80 to 20 °C. The difference spectra were calculated according to log (S_{last}/S_n), where S_n is the single-beam spectrum of the nth scan and S_{last} is the single-beam spectrum of the last scan.

ing and the results obtained from the stopped-flow measurements, experimental conditions were kept as similar as possible. Therefore, temperature-induced refolding of RNase A was monitored in the presence of 0.6 M [^{13}C]urea as well as in its absence. Figure 6 shows a series of difference spectra as obtained from a typical T-jump experiment carried out in the absence of the chaotropic agent. Difference spectra were computed from the single-beam spectra as described before for the stopped-flow experiments. It is interesting to note that the spectral refolding features of RNase A during the T-jump and during the stopped-flow experiments are very similar with respect to their relative band intensities and band positions (compare Figures 5 and 6).

From the difference spectra, intensity/time plots were generated for all kinetic measurements. Figure 7 presents the results obtained employing the prominent difference band at 1631 cm^{-1} as a probe for β-sheet structures, that emerge in response to the native conditions after stopped-flow dilution or T-jump, respectively. In all experiments, the intensity increase of this band exhibits typical exponential behavior. However, there are distinct differences between the kinetics of β-structure formation observed during the stopped-flow measurement in the presence of urea (Figure 7A) and during the T-jump experiment in the absence of the denaturant (Figure 7B). The β-structure refolds significantly faster (at least 2 times) in the absence of urea. This result is not surprising since the refolding conditions in the latter case are more native-like than in the presence of 0.6 M urea. Consequently, the refolding kinetics after a T-jump performed in the presence of urea should be slowed down compared to the urea-free experiment. Indeed, the results gained from such a measurement (Figure 7C) confirm this expectation. Moreover, the kinetics resemble those found in the stopped-flow experiment carried out at the same final concentration of urea. For all measurements, the intensity changes observed during the actual time window of 0.1−30 s correspond to 40−50% of the total effect observed in the equilibrium study. Therefore, about 50−60% of the total amount of β-sheet structure is regained either within the

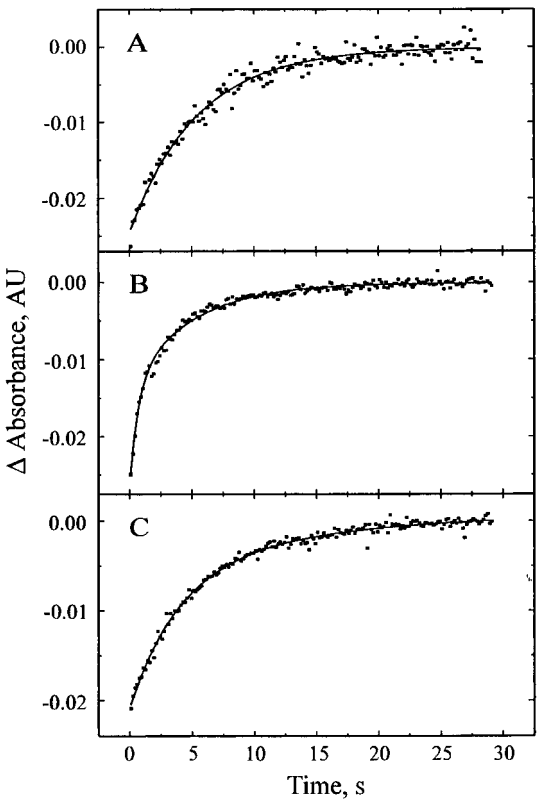

FIGURE 7: Refolding kinetics of RNase A monitored by time-resolved FTIR spectroscopy. Refolding was followed by measuring the amide I′ difference peak intensity at 1631 cm^{-1} as a function of time. (A) Stopped-flow experiment. (B) T-jump with RNase A in the absence of [^{13}C]urea. (C) T-jump with RNase A in the presence of [^{13}C]urea. Refolding conditions were 10 mg/mL RNase A, 0.6 M [^{13}C]urea (except in panel B), 20 mM sodium citrate/D_2O buffer, pH* 3.6, 20 °C. The solid lines represent exponential fits to the experimental data points.

experimental dead time (0 s < t < 0.1 s), indicating a further, much faster phase, or after ending of data acquisition (t > 30 s), that in turn would imply an additional slower phase. In fact, it is most likely that the formation of the "missing" amount of β-sheet splits up into both time ranges (see Discussion).

The experimental data were fitted with mono- or biphasic exponential decay functions. The averaged time constants and relative amplitudes of four individual experiments are summarized in Table 1. In 0.6 M urea, refolding of RNase A fits single exponential decay as indicated by the stopped-flow experiment and by the T-jump experiment in the presence of the denaturant. Furthermore, the time constants and amplitudes also coincide within the experimental error ($\tau = 6$ s, $\alpha = 40\%$). The formation of the β-sheet structures after initiation by a temperature jump in the absence of urea, on the other hand, exhibits biphasic character. The fitting procedure reveals two phases with time constants of 1.3 and 6.7 s, whereby the faster phase dominates with a ratio of the amplitudes of about 2:1 over the slower phase.

As shown in the equilibrium studies, infrared spectroscopy permits us not only to follow changes in the secondary structure in proteins but also to monitor the impact of unfolding and refolding on the microenvironment of certain side-chain groups, in particular of tyrosine. Unfortunately, the infrared bands of urea mask the conformation-sensitive ring stretching vibration of tyrosine at 1515 cm^{-1}. Therefore, the tyrosine band can only be analyzed during T-jump experiments in the absence of urea. Since the tyrosine signal

Table 1: Refolding Kinetics of RNase A Probed by the Absorbance Change of the β-Sheet Band at 1631 cm^{-1} and by the Frequency Change of the Tyrosine Ring Vibration at 1515 cm^{-1} under Different Experimental Conditions[a]

	IR "marker"	τ_1 (s)	α_1 (%)	τ_2 (s)	α_2 (%)	$t_{1/2}$ (s)	portion of total amplitude (%)
stopped-flow (0.6 M [^{13}C]urea)	β-band, 1631 cm^{-1}	5.9 ± 0.7	40 ± 4			4	40 ± 4
T-jump (without urea)	β-band, 1631 cm^{-1}	1.3 ± 0.5	31 ± 5	6.7 ± 1.3	17 ± 4	1.7	48 ± 4
	Tyr-band, 1515 cm^{-1}	5	60			3.5	60
T-jump (0.6 M [^{13}C]urea)	β-band, 1631 cm^{-1}	5.3 ± 0.6	41 ± 4			3.6	41 ± 4

[a] All measurements were done in 20 mM sodium citrate/D_2O, pH* 3.6 at 20 °C. The time constants, τ, and the amplitudes were obtained by fitting procedures with exponential decay functions. For the calculation of the relative amplitudes, α, the total changes of the corresponding marker bands under equilibrium conditions were set to 100%. The half-times, $t_{1/2}$, were estimated from the intensity/time plots to provide a better comparability of single phasic and biphasic kinetics. All values represent the average of four measurements. The standard deviations ($\pm$) are also given.

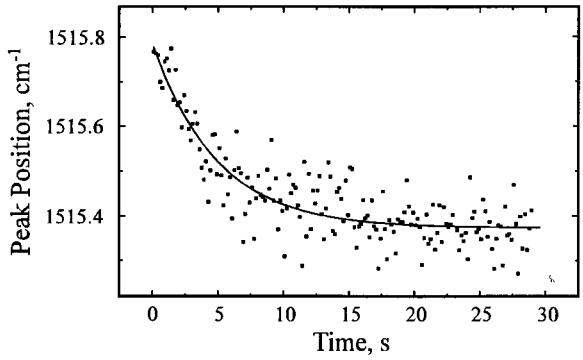

FIGURE 8: Shift of the peak position of the tyrosine ring vibration during the refolding of RNase A after a T-jump. Refolding conditions were the same as in Figure 7B except that a higher protein concentration of 25 mg/mL was used. Data points represent the average of four individual experiments. The solid line is the result of a monophasic exponential fit to the experimental points.

is very weak and the total shift is small (0.6 cm^{-1}), we have performed the T-jump experiments at higher protein concentrations of ~25 mg/mL but at otherwise identical conditions. It is important to note that the refolding kinetics of RNase A were not influenced by the higher protein concentration as proved from the intensity/time plots of the β-structure "marker" band at 1631 cm^{-1} (data not shown). Additionally, the data points of four individual experiments were averaged in order to improve the signal-to-noise ratio. This averaged tyrosine band frequency/time plot is given in Figure 8. Despite a relative high noise level, it can easily be seen that the shift of the tyrosine band during the thermally induced refolding occurs much slower ($\tau = 5$ s) than the absorbance change at 1631 cm^{-1} (compare Figures 7B and 8). Thus, under the strong native conditions applied in these experiments, the β-sheet structure in RNase A is formed before the tyrosine side chains adopt their native microenvironments.

DISCUSSION

Measurements under Equilibrium Conditions. The structural response of ribonuclease A to thermal and chemical disturbance was investigated under equilibrium conditions with FTIR spectroscopy. Several infrared bands employed as markers for the folding state of the polypeptide chain indicated a simple two-state equilibrium between folded and unfolded species. For a given experiment, the plots of different "markers" coincide with respect to the midpoints of the denaturation curves, T_m or $[urea]_{1/2}$, respectively. In agreement with data obtained by other techniques [see, e.g., Pace et al. (1990)], we therefore conclude that RNase A unfolds and refolds under equilibrium conditions in a highly cooperative process involving all structural components. This statement holds true for the thermal and the chemical perturbation. Furthermore, a comparative analysis of the amide I′ region of the infrared spectra of thermally and chemically denatured RNase A indicates that the different denaturating conditions lead to virtually identical unfolded states of this protein.

Comparison of RNase A Refolding Kinetics after Thermal and Chemical Denaturation. To the best of our knowledge, the application of the stopped-flow technique and the use of ^{13}C-labeled urea enabled us for the first time to monitor the kinetics of β-structure formation of a chemically denatured protein in real time by FTIR spectroscopy. By performing temperature jump experiments under strictly identical refolding conditions, it was also possible to compare directly the refolding rates and amplitudes of thermally and chemically unfolded RNase A in the time range from 100 ms to 30 s. Because unfolded RNase A consists of a mixture of conformational isomers arising from cis-trans isomerization reactions of the two native cis X−Pro peptide bonds in the unfolded molecule (Schmid, 1992), it was necessary to take care that the equilibrium ratio of all species was reached within the unfolding time. Proline isomerization in unfolded proteins is a very slow reaction, but as a consequence of its high activation energy, it is strongly temperature-dependent (Cook et al., 1979). The long unfolding duration in the case of the stopped-flow measurements (>10 h) and, on the other hand, the high unfolding temperature applied in the T-jump experiments during denaturation (80 °C) ensured that in both refolding experiments the same populations of unfolded species were employed. In this way, two essential prerequisites for the comparative analysis of chemically and thermally induced refolding were satisfied: identical populations of unfolded conformational isomers and identical refolding conditions. The fact that with these conditions practically identical refolding rates and amplitudes were obtained for the formation of β-structure in RNase A provides strong evidence for a high structural similarity of heat-denatured and urea-denatured RNase A. Any conformational differences between these states should affect their refolding kinetics. Since this is obviously not the case, our kinetic infrared studies perfectly corroborate the conclusions derived from the direct comparison of the infrared spectra of thermally and chemically denatured RNase A under equilibrium conditions published recently (Fabian & Mantsch, 1995) and those reported herein. Consequently, it is safe to conclude that the nature and amount of residual structure, if present at all, are identical for both unfolded states of RNase A.

Comparison of Thermally Induced Refolding in the Presence and Absence of [^{13}C]Urea. In T-jump experiments,

the refolding of heat-denatured RNase A was followed in the absence of urea as well as in its presence. The kinetics of β-sheet formation monitored at 1631 cm^{-1} were found to be significantly slowed down by the denaturant. Furthermore, in contrast to the thermally induced refolding in 0.6 M urea which obeyed single exponential kinetics, the same but urea-free experiment revealed biphasic refolding reactions. These results are consistent with the dependence of refolding rates of proteins on denaturant concentration that seems to be common for proteins [see, for a review, Baldwin (1996)]. Moreover, the appearance of additional refolding phases under strongly native conditions, as in the urea-free experiments, was also observed for some proteins (Kuwajima et al., 1989; Khorasanizadeh et al., 1996). This behavior can be attributed to kinetic intermediates, that accumulate during the folding process only under favorable refolding conditions, whereas they are destabilized and therefore not observed at higher denaturant concentrations (Schmid, 1992).

Tyrosine Vibration Monitors Formation of Tertiary Structure during Refolding. The position of the aromatic ring stretching mode of tyrosine at ~1515 cm^{-1}, used as a sensitive local monitor of protein conformation under equilibrium conditions (Fabian et al., 1994), was for the first time employed to follow also the kinetics of refolding. The comparative analysis of the kinetics of β-sheet formation with the time course of the tyrosine band shift revealed clear differences. In particular, tyrosine-detected refolding exhibited significant slower kinetics than refolding monitored by the amide I′ band component at 1631 cm^{-1}. This suggests that after β-structure formation there are still conformational changes detectable affecting the microenvironments of the tyrosine side chains. In the UV−VIS region, the tyrosine absorbance at 287 nm is often used to monitor the formation of tertiary structure, which for RNase A succeeds the formation of secondary structure (Udgaonkar & Baldwin, 1988). Similar conclusions can be drawn from the infrared data presented herein. It is therefore tempting to speculate that the tyrosine band shift observed in the infrared, on one side, and the UV absorbance change at 287 nm, on the other side, reflect the same molecular events during protein folding. In order to get an idea of what the molecular changes are that affect the microenvironments of the tyrosine side chains, a closer inspection of the three-dimensional structure of native RNase A was done using the program RasMol. Three of the six tyrosines in RNase A (Y25, Y73, and Y97) are known to be buried in the native molecule whereas the other three (Y76, Y92, and Y115) are located on the protein surface (Wlodawer & Sjölin, 1983). The visual inspection revealed that even the so-called solvent-exposed residues are at least partly shielded from water. Therefore, the hydrophobicity of the environment of all tyrosine side chains should become more or less affected during the folding process. An analysis of the atomic distances using the CCP4 program suite suggests a significant probability for all six tyrosines to be involved in intramolecular hydrogen bonding via their hydroxyl groups. It is interesting to note that none of the putative participating proton acceptors is located in the same structural element as the bound tyrosine residue is. Thus, these hydrogen bonds can only form when tertiary contacts are developed. The observed peak shift of the tyrosine infrared band during refolding of RNase A therefore seems to reflect both the formation of tertiary contacts and side chain packing interactions, whereby most likely all six tyrosine residues are more or less involved.

Comparison of Refolding Kinetics Studied by Infrared Spectroscopy and by NMR Hydrogen Exchange Experiments. In the refolding kinetics of RNase A, at least three parallel folding pathways which arise from a mixture of conformational isomers in the unfolded state are generally reported in literature. The cis-trans isomerizations of the two native cis prolyl prolyl bonds that occur in unfolded RNase A are thought to be responsible for this heterogeneity (Houry et al., 1994; Dodge & Scheraga, 1996). There is a fast-folding fraction, U_F, that is populated in equilibrium to 20%, and that refolds on the millisecond time-scale to the native enzyme, N. The slow-folding species, U_S, contains at least one incorrect proline isomer and divides up into two species, U_SI and U_SII, which account for 15 and 65% of unfolded RNase A, respectively. U_SI refolds in a very slow process on the minute time scale. The refolding pathway of the major unfolded form of RNase A (U_SII) has two kinetic intermediates: the early intermediate, I_1 (Schmid & Baldwin, 1979; Kim & Baldwin, 1980), and the late native-like intermediate, I_N (Cook et al., 1979; Schmid, 1983). The infrared spectroscopic approach developed and applied in the present work covers the time range from 100 ms to 30 s. Thus, refolding of the fast-folding species U_F cannot be observed because it occurs within the instrumental dead time. In addition, also the very slow folding species U_SI should not significantly contribute to the experimental data. Consequently, the observed spectral changes should primarily originate from the refolding of the major unfolded form U_SII, which accounts for ~65% of unfolded RNase A. In the present time range, we were able to monitor the refolding of 40−50% of the β-sheet system of RNase A. Most likely the difference to 65%, of 15−25%, is already regained within the experimental dead time.

The present infrared data are at variance to NMR experiments, which indicate that the entire β-sheet of RNase A is already formed in the early intermediate I_1 in less than 1 s as probed by the kinetics of hydrogen exchange protection (Udgaonkar & Baldwin, 1988, 1990). It is generally assumed that protection from hydrogen exchange monitors rapid formation and/or stabilization of secondary structure during refolding. Exactly the same is true for the infrared band at 1631 cm^{-1} that originates from carbonyl vibrations that are shifted from the typical random-coil absorption near 1650 cm^{-1} to the β-band position at 1631 cm^{-1} just as a result of the characteristic β-structure hydrogen bonding pattern. In this way, the IR band at 1631 cm^{-1} reflects directly the formation of the hydrogen bonding pattern when β-sheet structure is built up in RNase A. Therefore, one would expect comparable refolding kinetics monitored by the infrared and the NMR approach. In fact, however, the formation of the β-sheet in RNase A seems to proceed much faster when monitored by hydrogen exchange than when followed by TRIR spectroscopy. Discrepancies between pulsed hydrogen exchange experiments, on one side, and optical probes, on the other side, are not uncommon. Recent studies of several proteins have shown early folding intermediates with far-UV CD spectra that reflect the presence of large amounts of secondary structure at a stage where pulsed hydrogen exchange indicated the presence of no, or little, secondary structure (Elöve et al., 1992; Radford et al., 1992; Varley et al., 1993). It has been suggested that the secondary structure determined by CD could be the result of fluctuating structures which would not give a high degree

of hydrogen exchange protection (Guijarro, 1995). In the present case of RNase A, however, we note just the opposite, namely, a protection of amide protons located within the β-sheet of the native molecule very early during refolding, while the infrared data suggest a slower process of β-structure formation. A possible source for these discrepancies could be the nonidentical conditions applied during the pulse exchange and the IR measurements. In particular, it is not clear whether the conditions from which refolding starts after dilution of the denaturant are comparable between both types of experiments. In addition, most but not all backbone amide protons were used to monitor the folding of RNase A by NMR, and a few of the employed ones were found to be weakly or ill-defined protected (Udgaonkar & Baldwin, 1988, 1990), while the infrared spectra reflect all the backbone amide groups. Further work is needed to find the actual explanations for the conflicting results observed here by time-resolved infrared spectroscopy and previously by pulsed hydrogen exchange NMR experiments.

CONCLUSIONS

Since protein folding includes very different events that cover orders of magnitudes on the time-scale, it is important to have a variety of detection techniques that are sensitive to different inherent properties of the protein, and that complement each other with respect to their specific time window. The results reported herein show the feasibility of monitoring protein folding by time-resolved FTIR spectroscopy at a time resolution similar to those typical for well-known techniques such as stopped-flow CD or quenched flow hydrogen exchange. It is one of the strongest points of FTIR spectroscopy to have a complete spectrum available for each time point of measurement. In this way, several spectral windows are accessible to follow the formation of different secondary structure elements and also folding events that can be attributed to the formation of tertiary contacts. Thus, perfect time-correlation is ensured between folding events that can otherwise only be observed with different techniques, which often require different experimental conditions. One specific advantage of the infrared procedure is the ability to monitor directly the kinetics of β-sheet formation. This is exceptionally difficult to do with other techniques; far-UV CD-based techniques are more specific for α-helical structures, and pulse hydrogen exchange experiments provide the structural information in an indirect way. The new approach, combining stopped-flow or T-jump techniques and FTIR spectroscopy, has certainly a great potential to complement the established techniques in describing structural events that occur during protein folding and, therefore, should find a wide range of applications.

ACKNOWLEDGMENT

We thank Christopher W. Wharton for help in designing our stopped-flow equipment and for allowing us to use a stopped-flow cuvette designed by him. We are grateful to Dietmar Röleke for skillful assistance in crystallographic data analysis.

REFERENCES

Akasaka, K., Naito, A., & Nakatani, H. (1991) *J. Biomol. NMR 1*, 65−70.

Backmann, J., Fabian, H., & Naumann, D. (1995) *FEBS Lett. 364*, 175−178.

Balbach, J., Forge, V., van Nuland, N. A. J., Winder, S. L., Hore, P. J., & Dobson, C. M. (1995) *Nat. Struct. Biol. 2*, 865−870.

Baldwin, R. L. (1996) *Folding Des. 1*, R1−R8.

Chaffotte, A. F., Guillou, Y., & Goldberg, M. E. (1992) *Biochemistry 31*, 9694−9702.

Cook, K. H., Schmid, F. X., & Baldwin, R. L. (1979) *Proc. Natl. Acad. Sci. U.S.A. 76*, 6157−6161.

Dodge, R. W., & Scheraga, H. A. (1996) *Biochemistry 35*, 1548−1559.

Elöve, G. A., Chaffotte, A. F., Roder, H., & Goldberg, M. E. (1992) *Biochemistry 31*, 6876−6883.

Fabian, H., & Mantsch, H. H. (1995) *Biochemistry 34*, 13651−13655.

Fabian, H., Schultz, C., Naumann, D., Landt, O., Hahn, U., & Saenger, W. (1993) *J. Mol. Biol. 232*, 967−981.

Fabian, H., Schultz, C., Backmann, J., Hahn, U., Saenger, W., Mantsch, H. H., & Naumann, D. (1994) *Biochemistry 33*, 10725−10730.

Fischer, D., Rice, D., Bowie, J. U., & Eisenberg, D. (1996) *FASEB J. 10*, 126−136.

Glasoe, P. K., & Long, F. A. (1960) *J. Phys. Chem. 64*, 188−190.

Guijarro, J. I., Jackson, M., Chaffotte, A. F., Mantsch, H. H., & Goldberg, M. E. (1995) *Biochemistry 34*, 2998−3008.

Haris, P. I., Lee, D. C., & Chapman, D. (1986) *Biochim. Biophys. Acta 874*, 255−265.

Houry, W. A., Rothwarf, D. M., & Scheraga, H. A. (1994) *Biochemistry 33*, 2516−2530.

Jackson, M., & Mantsch, H. H. (1995) *Crit. Rev. Biochem. Mol. Biol. 30*, 95−120.

Jeng, M.-F., Englander, S. W., Elöve, G. A., Wand, A. J., & Roder, H. (1990) *Biochemistry 29*, 10433−10437.

Khorasanizadeh, S., Peters, I. D., & Roder, H. (1996) *Nat. Struct. Biol. 3*, 193−205.

Kim, P. S., & Baldwin, R. L. (1980) *Biochemistry 19*, 6124−6129.

Kuwajima, K., Mitani, M., & Sugai, S. (1989) *J. Mol. Biol. 206*, 547−561.

Levinthal, C. (1968) *J. Chim. Phys. 65*, 44−45.

Makhatadze, G. I., Clore, G. M., & Gronenborn, A. M. (1995) *Nat. Struct. Biol. 2*, 852−855.

Mullins, L. S., Pace, C. N., & Raushel, F. M. (1993) *Biochemistry 32*, 6152−6156.

Olinger, J. M., Hill, D. M., Jakobsen, R. J., & Brody, R. S. (1986) *Biochim. Biophys. Acta 869*, 89−98.

Pace, C. N. (1986) *Methods Enzymol. 131*, 266−280.

Pace, C. N., Laurents, D. V., & Thomson, J. A. (1990) *Biochemistry 29*, 2564−2572.

Phillips, C. M., Mizutani, Y., & Hochstrasser, R. M. (1995) *Proc. Natl. Acad. Sci. U.S.A. 92*, 7292−7296.

Privalov, P. L., & Khechinashvili, N. N. (1974) *J. Mol. Biol. 86*, 665−684.

Radford, S. E., Dobson, C. M., & Evans, P. A. (1992) *Nature 358*, 302−307.

Schmid, F. X. (1983) *Biochemistry 22*, 4690−4696.

Schmid, F. X. (1992) in *Protein Folding* (Creighton, T. E., Ed.) pp 197−241, Freeman Press, New York.

Schmid, F. X., & Baldwin, R. L. (1979) *J. Mol. Biol. 135*, 199−215.

Tanford, C. (1968) *Adv. Protein Chem. 23*, 122−283.

Udgaonkar, J. B., & Baldwin, R. L. (1988) *Nature 335*, 694−699.

Udgaonkar, J. B., & Baldwin, R. L. (1990) *Proc. Natl. Acad. Sci. U.S.A. 87*, 8197−8201.

Udgaonkar, J. B., & Baldwin, R. L. (1995*) Biochemistry 34*, 4088−4096.

Varley, P., Gronenborn, A. M., Christensen, H., Wingfield, P. T., Pain, R. H., & Clore, G. M. (1993) *Science 260*, 1110−1113.

White, A. J., Drabble, K., & Wharton, C. W. (1995) *Biochem. J. 306*, 843−849.

Williams, S., Causgrove, T. P., Gilmanshin, R., Fang, K. S., Callender, R. H., Woodruff, W. H., & Dyer, R. B. (1996) *Biochemistry 35*, 691−697.

Wlodawer, A., & Sjölin, L. (1983) *Biochemistry 22*, 2720−2728.

BI961810J